Spectral and optical properties in the antiphase stripe phase of the cuprate superconductors

2009 J. Phys.: Condens. Matter 21 375701

(http://iopscience.iop.org/0953-8984/21/37/375701)

J. Phys.: Condens. Matter **21** (2009) 375701 (7pp) doi:10.1088/0953-8984/21/37/375701

Spectral and optical properties in the antiphase stripe phase of the cuprate superconductors

Hong-Min Jiang, Cui-Ping Chen and Jian-Xin Li

National Laboratory of Solid State of Microstructure and Department of Physics, Nanjing University, Nanjing 210093, People's Republic of China

Received 5 May 2009
Published 17 August 2009
Online at stacks.iop.org/JPhysCM/21/375701

Abstract

We investigate the superconducting order parameter, the spectral and optical properties in a stripe model with spin-(charge-) domain-derived scattering potential V_s (V_c). We show that the charge-domain-derived scattering is less effective than the spin scattering on the suppression of superconductivity. For $V_s \gg V_c$, the spectral weight concentrates on the $(\pi, 0)$ antinodal region and a finite energy peak appears in the optical conductivity with the disappearance of the Drude peak. But for $V_s \approx V_c$, the spectral weight concentrates on the $(\pi/2, \pi/2)$ nodal region and a residual Drude peak exists in the optical conductivity without the finite energy peak. These results consistently account for the divergent observations in the ARPES and optical conductivity experiments in several high-T_c cuprates and suggest that the 'insulating' and 'metallic' properties are intrinsic to the stripe state, depending on the relative strength of the spin- and charge-domain-derived scattering potentials.

(Some figures in this article are in colour only in the electronic version)

1. Introduction

The nature of spin and/or charge inhomogeneities, especially in the form of stripes, in some cuprates and their involvement in high-temperature superconductivity are currently debated issues [1]. The stripe state is characterized by the self-organization of the charges and spins in the CuO_2 planes in a peculiar manner, where the doped holes are arranged in one-dimensional (1D) lines and form the so-called 'charge stripe' separating the antiferromagnetic domains. The stripe-ordered state minimizes the energy of the hole-doped antiferromagnetic system, thus leading to an inhomogeneous state of matter. Static one-dimensional charge and spin stripe order have been observed experimentally in a few special cuprate compounds, specifically in $La_{1.6-x}Nd_{0.4}Sr_xCuO_4$ [2, 3] and $La_{2-x}Ba_xCuO_4$ with $x = 1/8$ [5, 4]. Similar signatures identified in $La_{2-x}Sr_xCuO_4$ (LSCO) [6–9] and other high-temperature superconductors [10–12] point to the possible existence of stripes, albeit of a dynamical or fluctuating nature.

A pivotal issue about this new electronic state of matter concerns whether it is compatible with superconductivity, and possibly even essential for the high transition temperatures, or if it competes with the pairing correlations. A prerequisite for addressing these issues is to understand the electronic structures of various stripe states in different cuprates, and to answer the question whether the stripe phase is intrinsically 'metallic' or 'insulating', given its spin- and charge-ordered nature. An angle-resolved photoemission spectroscopy (ARPES) study by Zhou *et al* in $(La_{1.28}Nd_{0.6}Sr_{0.12})CuO_4$ with static stripes has found the depletion of the low-energy excitation near the $(\pi/2, \pi/2)$ nodal region [3]. In another compound $La_{1.875}Ba_{0.125}CuO_4$, a system where the superconductivity is heavily suppressed due to the development of the static spin and charge orders, Valla *et al* and He have detected the high spectral intensity of the low-energy excitation in the vicinity of the $(\pi/2, \pi/2)$ nodal region [13, 14]. The compound $(La_{1.4-x}Nd_{0.6}Sr_x)CuO_4$ ($x = 0.10$ and 0.15), with a static one-dimensional stripe, seems to be an in-between system, in where the existence of spectral weight around the nodal region, though weak, has been identified [15].

Meanwhile, optical conductivity measurements on the systems with a stripe phase also display the divergent results. In $La_{1.275}Nd_{0.6}Sr_{0.125}CuO_4$ [16] and $La_{1.875}Ba_{0.125-x}Sr_xCuO_4$ [17], a finite frequency absorption peak with the almost disappearance of the Drude mode in the low-frequency

conductivity in several experiments has been interpreted as collective excitations of charge stripes or as charge localization from the disorder created by Nd or Ba substitutions. These observations may support the suggestion that such a stripe-ordered state should be 'insulating' in nature [18]. On the other hand, optical experiments on $La_{1.875}Ba_{0.125}CuO_4$ [19] have observed a residual Drude peak with a loss of the low-energy spectral weight below the temperature corresponding to the onset of charge stripe order, which indicates that stripes are compatible with the so-called nodal-metal state [20–24, 19].

Although there have been some theoretical studies on the spectral and optical properties in the stripe phase in the past years [25–28], the contradictory observations in recent experiments as mentioned above have not yet been explained consistently in a theoretical framework by adopting a realistic stripe model. In this paper, by using a stripe model in which the experimentally observed spin and charge structures at 1/8 doping are well reflected, we show that the spin-domain-derived scattering will depress the zero-energy spectral weight around the nodal regions, while the charge-domain-derived scattering will suppress mostly those around the antinodal regions and the hot spots. Compared to the ARPES data, this suggests that the different spectral weight distribution may result from the different relative strengths of the spin- and charge-domain-derived scattering potentials inherently existing in these compounds. Meanwhile, a finite frequency peak in the optical conductivity appears with the disappearance of the Drude peak in the case of the dominant spin-domain-derived scattering, while a residual Drude peak exists with the disappearance of the finite energy peak when the charge-domain-derived scattering is comparable to the spin one. This suggests that both the 'insulating' and 'metallic' properties are intrinsic to the stripe state without introducing another distinct metallic phase.

The rest of this paper is organized as follows. In section 2, we introduce the model Hamiltonian and carry out the analytical calculations. In section 3, we present the numerical calculations and discuss the results. In section 4, we present the conclusion.

2. Theory and method

As the above-discussed compounds have a doping density at or near 1/8, in this paper we will consider the 1/8 doping antiphase vertical stripe state. A schematic illustration of its charge and spin pattern is presented in figure 1. The charge stripes, with a unit cell of 8 lattice sites (note for 1/8 doping, there is one hole for every two sites along the length of a charge stripe), act as antiphase domain walls for the magnetic order, so that the magnetic unit cell is twice as long as that for the charge order. Due to the periodical modulation of the stripe order, the electrons moving in the state will be scattered by the modulation potentials. After Fourier transformation, the potential V_n can be written as the scattering term between the state k and those at $k \pm nQ$ with $Q = (3\pi/4, \pi)$. Following [29], we expect that the terms V_1 and V_2 will be the dominant spin- and charge-domain-derived scattering term, and will be relabeled as V_s and V_c in the following, respectively. The weaker higher harmonic terms will be neglected here. In the coexistence with the superconducting (SC) order, the model Hamiltonian can be written as a 16×16 matrix for k in the reduced Brillouin zone:

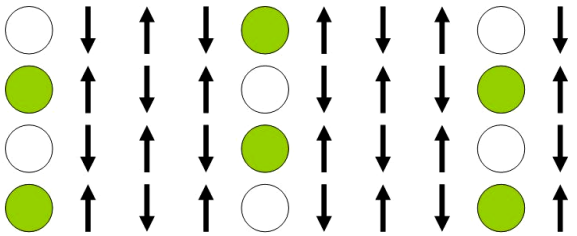

Figure 1. Schematic illustration of the charge and spin patterns in the 1/8-doped antiphase stripe state. Circles represent the charge-domain wall (an empty circle indicates a hole density of one per site) and arrows the copper spins.

$$\hat{H} = \sum_k{}' \hat{C}^\dagger(k) \begin{pmatrix} \hat{H}_k & \hat{\Delta}_k \\ \hat{\Delta}_k & -\hat{H}_k \end{pmatrix} \hat{C}(k), \tag{1}$$

where the prime denotes the summation over the reduced Brillouin zone. $\hat{C}_k$ is a column vector with its elements $C_i(k) = C_{k+(i-1)Q,\uparrow}$ for $i = 1, 2, \ldots, 8$ and $C^\dagger_{-k-(i-9)Q,\downarrow}$ for $i = 9, 10, \ldots, 16$. Both $\hat{H}_k$ and $\hat{\Delta}_k$ are 8×8 matrices with

$$\hat{H}_k = \begin{pmatrix} \varepsilon_k & V_s & V_c & 0 & 0 & 0 & V_c & V_s \\ V_s & \varepsilon_{k+Q} & V_s & V_c & 0 & 0 & 0 & V_c \\ V_c & V_s & \varepsilon_{k+2Q} & V_s & V_c & 0 & 0 & 0 \\ 0 & V_c & V_s & \varepsilon_{k+3Q} & V_s & V_c & 0 & 0 \\ 0 & 0 & V_c & V_s & \varepsilon_{k+4Q} & V_s & V_c & 0 \\ 0 & 0 & 0 & V_c & V_s & \varepsilon_{k+5Q} & V_s & V_c \\ V_c & 0 & 0 & 0 & V_c & V_s & \varepsilon_{k+6Q} & V_s \\ V_s & V_c & 0 & 0 & 0 & V_c & V_s & \varepsilon_{k+7Q} \end{pmatrix}, \tag{2}$$

and

$$\hat{\Delta}_k = \begin{pmatrix} \Delta_k & 0 & 0 & 0 & 0 & 0 & 0 & 0 \\ 0 & \Delta_{k+Q} & 0 & 0 & 0 & 0 & 0 & 0 \\ 0 & 0 & \Delta_{k+2Q} & 0 & 0 & 0 & 0 & 0 \\ 0 & 0 & 0 & \Delta_{k+3Q} & 0 & 0 & 0 & 0 \\ 0 & 0 & 0 & 0 & \Delta_{k+4Q} & 0 & 0 & 0 \\ 0 & 0 & 0 & 0 & 0 & \Delta_{k+5Q} & 0 & 0 \\ 0 & 0 & 0 & 0 & 0 & 0 & \Delta_{k+6Q} & 0 \\ 0 & 0 & 0 & 0 & 0 & 0 & 0 & \Delta_{k+7Q} \end{pmatrix}. \tag{3}$$

As for the tight-binding energy band, we will choose the following form [30, 31]:

$$\varepsilon_k = -2(\delta t + J'\chi_0)(\cos k_x + \cos k_y) - 4\delta t' \cos k_x \cos k_y - \mu. \tag{4}$$

where δ is the doping density and a d-wave SC order parameter $\Delta_k = 2J'\Delta_0(\cos k_x - \cos k_y)$ is assumed. Generally, the charge modulation will induce the modulation of the SC order leading to the finite momentum pairs. However, in the present

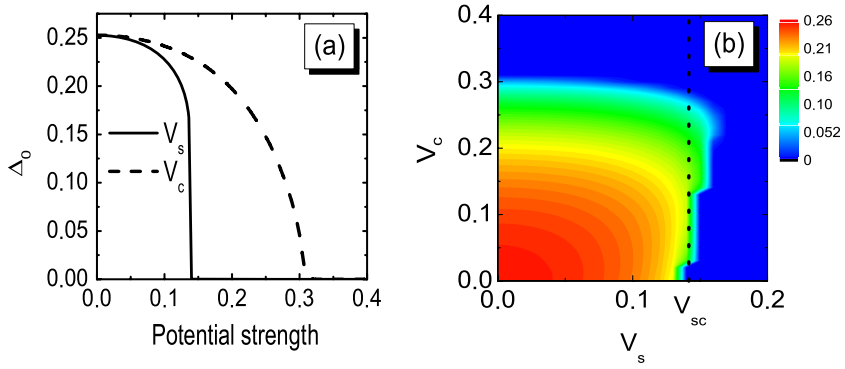

Figure 2. (a) Superconducting order parameter as a function of V_s and V_c, respectively. (b) A two-dimensional map of the superconducting order parameter in the parameter space of V_s and V_c.

study, one of our aims is to examine the effect of the spin-(charge-) domain-derived scattering on the SC order. In this regard, the average value of the SC order parameter is relevant and the modulation of the SC order will be ignored. We have checked the effect of this modulation and found no qualitative change in the results presented in figure 2. In the following, $J = 100$ meV is taken as the energy unit, $t = 2J, t' = -0.45t$ and $J' = \frac{3}{8}J$. This dispersion can be derived from the slave-boson mean-field calculation of the $t - t' - J$ model [30, 31] and, in this way, the parameters Δ_0, χ_0 and μ are determined self-consistently. Here we take it as a phenomenological form. In a self-consistent calculation, the Hamiltonian is first diagonalized by a unitary matrix $\hat{U}(k)$ with a set of trial values of Δ_0, χ_0 and μ for given potentials V_s and V_c. Then Δ_0, χ_0 and μ are self-consistently calculated by using the relations: $\pm\Delta_0 = \langle c_{i\uparrow}c_{i+\tau\downarrow} - c_{i\downarrow}c_{i+\tau\uparrow}\rangle$ (To get the d-wave pairing, the sign before Δ_0 takes $+$ for $\tau = \pm\hat{x}$ and $-$ for $\tau = \pm\hat{y}$, where $\hat{x}$ and $\hat{y}$ denote the unit vectors along the x and y directions, respectively.), $\chi_0 = \sum_\sigma \langle c^\dagger_{i\sigma}c_{j\sigma}\rangle$ and $n = \sum_\sigma \langle c^\dagger_{i\sigma}c_{i\sigma}\rangle$, respectively. Reformularization of the expressions of Δ_0, χ_0 and μ in terms of eigenfunctions and eigenvalues of the Hamiltonian, one obtains the self-consistency relations

$$\Delta_0 = -\frac{1}{N}\sum_k(\cos k_x - \cos k_y)\sum_{m=1}^{16} U_{1m}(k)U^\dagger_{m9}(k) \times f[E_m(k)]$$

$$\chi_0 = \frac{1}{N}\sum_k(\cos k_x + \cos k_y)\sum_{m=1}^{16} U_{1m}(k)U^\dagger_{m1}(k) \times f[E_m(k)] \quad (5)$$

$$n = \frac{2}{N}\sum_k\sum_{m=1}^{16} U_{1m}(k)U^\dagger_{m1}(k)f[E_m(k)],$$

where $E_m(k)$ is the eigenvalue of the Hamiltonian, $U_{mn}(k)$ are the elements of the matrix $\hat{U}(k)$ and $f[E_m(k)]$ is the Fermi–Dirac distribution function.

Then, the single-particle Green functions $G_{ij}(k, \mathrm{i}\omega_n) = -\int_0^\beta \mathrm{d}\tau \exp^{\mathrm{i}\omega_n\tau}\langle T_\tau C_i(k, \mathrm{i}\tau)C^\dagger_j(k, 0)\rangle$ can be expressed as

$$G_{ij}(k, \mathrm{i}\omega_n) = \sum_{m=1}^{16}\frac{U_{im}(k)U^\dagger_{mj}(k)}{\mathrm{i}\omega_n - E_m(k)}, \quad (6)$$

and the spectral function is

$$A_{ij}(k, \omega) = -\frac{1}{\pi}\,\mathrm{Im}\,G_{ij}(k, \omega + \mathrm{i}0^+). \quad (7)$$

3. Results and discussion

3.1. Self-consistent calculation of the SC order parameter

We first present in figure 2 the self-consistent results of the SC order parameter as a function of V_s and V_c. While the scattering from both spin- and charge-domain-derived scattering potentials in the stripe state leads to the suppression of the SC order parameter, the charge domains are more compatible with superconductivity than spin domains, as can be seen from figure 2(a). This may support the statement that the SC pairing in the stripe state occurs most strongly within the charge stripes [32]. On the other hand, an interesting feature is that the SC order parameter will be zero at the spin-domain-derived scattering potential $V_{sc} \approx 0.14$ in the absence of the charge-domain-derived scattering: however, it will develop a noticeable value after turning on the charge-domain-derived scattering potential, as shown in figure 2(b). This shows that the charge-domain-derived scattering will lead to the emergence of the SC order which is otherwise destroyed by the spin-only scattering.

3.2. Distribution of spectral weight

In figure 3, we present the distribution of the low-energy spectral weight in the original Brillouin zone (integrated over an energy window $\Delta\epsilon = 0.1J$ about ϵ_F) in the 1/8 antiphase stripe state for different spin-(charge-) domain-derived scattering potential V_s (V_c). Let us first look at the limit where only the spin-domain-derived scattering is included, i.e. $V_c = 0$ with $V_s = 0.15$. One will find that the spectral weight around the nodal region is suppressed heavily (see figure 3(a)). At another limit where only the charge-domain-derived scattering is included ($V_c = 0.17$ with $V_s = 0$), the spectral weight around the nodal region is recovered and those around the hot spot (the crossing of the Fermi surface with the line $k_x \pm k_y = \pm\pi$) and near the antinodal region are suppressed (see figure 3(b)). Starting

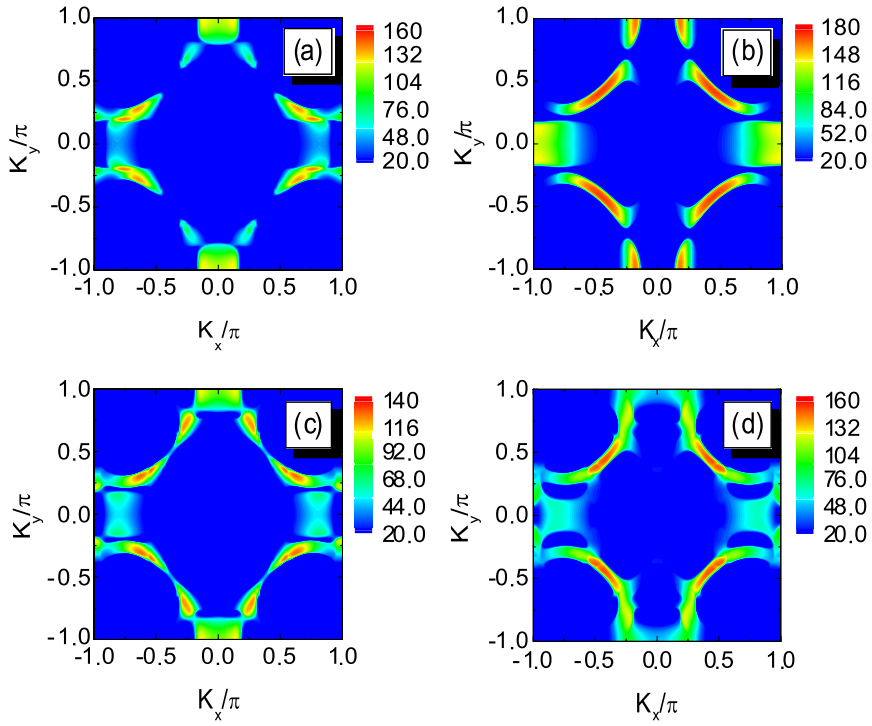

Figure 3. Spectral weight distribution for different spin-(charge-) domain-derived scattering potentials in the normal state with (a) $V_s = 0.15$ and $V_c = 0$, (b) $V_s = 0$ and $V_c = 0.17$, (c) $V_s = 0.15$ and $V_c = 0.08$, and (d) $V_s = 0.15$ and $V_c = 0.17$, respectively.

from the limit of $V_c = 0$ and fixing $V_s = 0.15$, the spectral weight will redistribute gradually from the antinodal region to the nodal region with the increase of the charge-domain-derived scattering potential V_c, as shown in figures 3(c) and (d). When two scattering potentials are comparable, the strongest spectral weight is situated around the nodal region, and in the meantime noticeable spectral weights along the whole Fermi surface are presented. Therefore, the divergent features observed in ARPES measurements by Zhou *et al* in $(La_{1.28}Nd_{0.6}Sr_{0.15})CuO_4$ [15] in which the low-energy excitations near the nodal region are depleted, and by Valla *et al* in $La_{1.875}Ba_{0.125}CuO_4$ [13, 14] in which the high spectral intensity of the low-energy excitation in the vicinity of the nodal region is detected, are consistently reproduced here by a change of the relative strength between the charge- and spin-domain-derived scattering. This consistent accounting enables us to propose that the spin-domain-derived scattering dominates over the charge one in the former system while the scattering strengths of them are comparable in the latter system.

In the presence of the spin-(charge-) domain-derived potential, quasiparticles near the Fermi surface will be scattered from $\mathbf{k}$ to $\mathbf{k} \pm n\mathbf{Q}$ ($n = 1$ for the spin-domain-derived potential, $n = 2$ for the charge one), for the 1/8 antiphase vertical stripe configuration shown as figure 1. This gives rise to two scattering channels from the spin domain with potential V_s:

$$\begin{aligned} \mathbf{k} &\to \mathbf{k} + Q = \mathbf{k} + (3\pi/4, \pi), \\ \mathbf{k} &\to \mathbf{k} - Q = \mathbf{k} + (5\pi/4, \pi), \end{aligned} \tag{8}$$

and two scattering channels from the charge domain with potential V_c:

$$\begin{aligned} \mathbf{k} &\to \mathbf{k} + 2Q = \mathbf{k} + (3\pi/2, 0), \\ \mathbf{k} &\to \mathbf{k} - 2Q = \mathbf{k} + (\pi/2, 0). \end{aligned} \tag{9}$$

Strong potential scattering will destroy those parts of the Fermi surface connected by the above-mentioned scattering wavevectors. Because the scattering wavevectors Q and $-Q$ are close to the transferred momenta from the node to node scattering, it will lead to a depletion of the spectral weight near the nodal region as shown in figure 3(a). On the other hand, for the scattering wavevectors $2Q$ and $-2Q$, which are near the connecting wavevectors between the two approximately parallel segments of the Fermi surface near the antinodal and hot spot region, the scatterings with these wavevectors will suppress the spectral weights around the antinodal and hot spot regions (figure 3(b)).

3.3. In-plane optical conductivity

Now, we turn to the discussion of the in-plane optical properties in the 1/8 antiphase stripe state and to see how they are influenced by the scattering from the spin and charge domains. We will fix the temperature at $T = 0.05$ in all calculations in order to avoid the influence from the temperature-induced change in the scattering rate. We consider an electric field applied in the x direction, which is perpendicular to the stripe. From the Kubo formula for the optical conductivity, the real part of the optical conductivity is $\sigma_1(\omega) = -\lim_{q\to 0} \mathrm{Im}[\Pi(q, \omega)]/\omega$. The imaginary part of

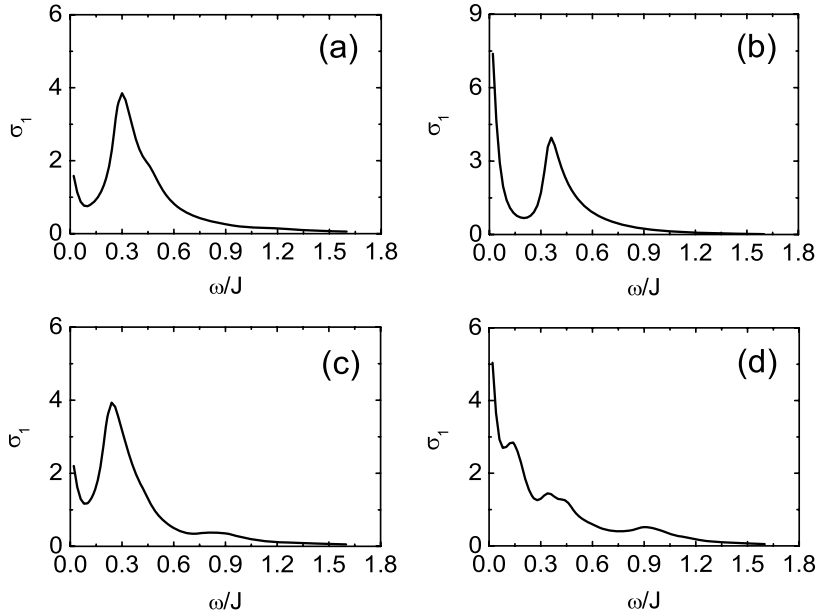

Figure 4. In-plane optical conductivity as a function of frequency for different spin-(charge-) domain-derived scattering potentials in the 1/8 antiphase stripe with the SC order parameter $\Delta = 0$. (a) $V_s = 0.15$ and $V_c = 0$, (b) $V_s = 0$ and $V_c = 0.17$, (c) $V_s = 0.15$ and $V_c = 0.08$, and (d) $V_s = 0.15$ and $V_c = 0.17$.

the current–current correlation function $\mathrm{Im}[\Pi(q \to 0, \omega)]$ is given by

$$\mathrm{Im}[\Pi(q \to 0, \omega)] = \frac{\pi}{N} \sum_{k}{}' \sum_{j,l=1}^{16} v^{jj}(k) v^{ll}(k) \times \int \mathrm{d}\omega' [f(\omega + \omega') - f(\omega')] \times A_{jl}(k, \omega') A_{lj}(k, \omega + \omega'). \quad (10)$$

Here, $v^{jj}(k)$ is the diagonal element of the quasiparticle group velocity in the matrix form:

$$\hat{v}(k) = \begin{pmatrix} \frac{\partial \hat{H}_k}{\partial k_x} & 0 \\ 0 & -\frac{\partial \hat{H}_k}{\partial k_x} \end{pmatrix}. \quad (11)$$

Figures 4(a)–(d) show the results for the optical conductivity calculated with the same scattering potentials as used to get figures 3(a)–(d). With only spin-domain-derived scattering (figure 4(a)), no Drude-like component appears at zero frequency in the optical conductivity, instead, a finite frequency conductivity peak occurs around 0.3. This indicates that the system exhibits the 'insulating' property[1]. When only charge-domain-derived scattering is considered (figure 4(b)), the Drude-like peak shows up and, in the meantime, the finite frequency peak remains. Optical conductivity involves the contribution from the quasiparticle excitations along the whole Fermi surface weighted by the quasiparticle group velocity. Due to the relative flat band structure near the antinodal region for the high-T_c cuprates, the zero-frequency optical conductivity mainly comes from the quasiparticle excitations around the nodal region. In the case of only spin-domain-derived scattering, the nodal region of the Fermi surface is gapped and therefore the quasiparticle spectral weight is suppressed around the nodal region, as shown in figure 3(a), so that the zero-frequency Drude-like peak is absent and a finite frequency peak with its position being equal to the gap ($\approx 2V_s = 0.3$) occurs. For the charge-domain-derived scattering, the gap opens around the hot spots and near the antinodal, but a large spectral weight is situated around the nodal region, as can be seen from figure 3(b). Thus, the Drude-like peak emerges and the finite frequency peak remains (it is now situated at $\approx 2V_c = 0.34$). As shown in figure 3(c), with the increase of the charge-domain-derived scattering V_c, the gap near the nodal region which resulted from the spin-domain-derived scattering will be suppressed gradually and correspondingly the spectral weight will be enhanced. As a result, the finite frequency peak in the optical conductivity is shifted to lower frequency and the zero-frequency component is lifted up gradually (figure 4(c)). When the charge-domain-derived scattering is comparable to the spin one, the quasiparticles have noticeable spectra weight along the entire Fermi surface with its largest weight around the nodal region (figure 3(d)). Then the Drude-like mode occurs at the zero frequency and the finite frequency peak fades away and merges into the Drude-like peak, as shown in figure 4(d). The calculated results for the optical conductivity presented in figures 4(c) and (d) are well consistent with the experimental observations in the stripe states of $La_{1.275}Nd_{0.6}Sr_{0.125}CuO_4$ [16] and $La_{1.875}Ba_{0.125}CuO_4$ [19], respectively.

3.4. Discussion

We now discuss the implication of our theoretical results. As noted in section 1, in the $La_{1.275}Nd_{0.6}Sr_{0.125}CuO_4$ system,

[1] The term 'insulating' state used here follows [15, 17, 19] to indicate a strong suppression of Drude peak in the optical conductivity. In fact, the spectral weight at the Fermi level will not be fully gapped out, so it is not a true insulating state. We use the term here is to facilitate our comparison with the experiments [15, 17, 19].

the ARPES experiment has found that there is little or no low-energy spectral weight near the nodal region [3] and the optical conductivity experiment has observed a finite frequency peak with almost the disappearance of the Drude mode, indicating an 'insulating' stripe state [16, 17]. These spectroscopic features can be reproduced here with a strong spin-domain-derived scattering potential $V_s = 0.15$ and a weak charge-domain-derived potential $V_c = 0.08$ and $V_c = 0$, as shown in figures 3(a), (c), 4(a) and (c). Interestingly, in this parameter regime for the spin- and charge-domain-derived scattering, the SC order is destroyed, as can be seen from figure 2(b). This is consistent with the experimental fact that $La_{1.275}Nd_{0.6}Sr_{0.125}CuO_4$ is nonsuperconducting. In another cuprate $La_{1.875}Ba_{0.125}CuO_4$, ARPES spectra have identified the existence of high spectral intensity around the nodal region [13, 14] and the optical conductivity measurement has observed a residual Drude peak without the finite frequency peak [19], pointing to a so-called nodal-metal state [20–24, 19]. When comparable spin- and charge-domain-derived scattering potentials are assumed, such as $V_s = 0.15$ and $V_c = 0.17$, we can reproduce these features consistently, as shown in figures 3(d) and (d). On the other hand, a weak superconductivity emerges in the otherwise nonsuperconducting regime (when only the spin scattering potential V_{sc} is considered) with the increase of the charge-domain-derived scattering potential (see figure 2(b)). This suggests that the weak superconductivity in $La_{1.875}Ba_{0.125}CuO_4$ is likely beneficial from the metallic behaviors of the stripe state originating from a sufficient charge-domain-derived scattering. The above-mentioned consistent accounting for both divergent spectroscopic features observed in two families of high-T_c cuprates indicates that the stripe state may be intrinsically 'insulating' or 'metallic', depending on the relative strength of the spin- and charge-domain-derived scattering potentials. Specifically, a large spin-domain-derived scattering potential favors the 'insulating' state, while a large charge-domain-derived scattering potential the 'metallic' state.

4. Conclusion

We have calculated the SC order parameter, the spectral function and the optical conductivity in a stripe model with spin- and charge-domain-derived scattering potentials (V_s and V_c). The self-consistent calculation of the SC order parameter shows that the charge-domain-derived scattering is less effective than the spin scattering in the suppression of superconductivity, and may even lead to the emergence of the SC order which is otherwise destroyed by the spin-only scattering. For $V_s \gg V_c$, the zero-energy spectral weight disappears around the nodal points and a finite energy peak appears in the optical conductivity with almost the disappearance of the Drude peak. But for $V_s \approx V_c$, the spectral weight concentrates on the nodal region and a residual Drude peak exists in the optical conductivity without the finite energy peak. These results consistently account for the divergent spectroscopic properties observed experimentally in two families of high-T_c cuprates and demonstrate that both the 'insulating' and 'metallic' behavior may be intrinsic properties of the stripe state, depending on the relative strength of the spin- and charge-domain-derived scattering potentials.

Acknowledgments

This project was supported by the National Natural Science Foundation of China (grant no. 10525415), the Ministry of Science and Technology of Science (grant nos. 2006CB601002 and 2006CB921800), the China Postdoctoral Science Foundation (grant no. 20080441039) and the Jiangsu Planned Projects for Postdoctoral Research Funds (grant no. 0801008C).

References

[1] Kivelson S A, Bindloss I P, Fradkin E, Oganesyan V, Tranquada J M, Kapitulnik A and Howald C 2003 *Rev. Mod. Phys.* **75** 1201
[2] Tranquada J M, Sternlieb B J, Axe J D, Nakamura Y and Uchida S 1995 *Nature* **375** 561
[3] Zhou X J, Bogdanov P, Kellar S A, Noda T, Eisaki H, Uchida S, Hussain Z and Shen Z-X 1999 *Science* **286** 268
[4] Tranquada J M, Woo H, Perring T G, Goka H, Gu G D, Xu G, Fujita M and Yamada K 2004 *Nature* **429** 534
[5] Abbamonte P, Rusydi A, Smadici S, Gu G D, Sawatzky G A and Feng D L 2005 *Nat. Phys.* **1** 155
[6] Cheong S-W, Aeppli G, Mason T E, Mook H, Hayden S M, Canfield P C, Fisk Z, Clausen K N and Martinez J L 1991 *Phys. Rev. Lett.* **67** 1791
[7] Mason T E, Aeppli G and Mook H A 1992 *Phys. Rev. Lett.* **68** 1414
[8] Bianconi A, Saini N L, Lanzara A, Missori M, Rossetti T, Oyanagi H, Yamaguchi H, Oka K and Ito T 1996 *Phys. Rev. Lett.* **76** 3412
[9] Yamada K *et al* 1998 *Phys. Rev.* B **57** 6165
[10] Wells B O, Lee Y S, Kastner M A, Christianson R J, Birgeneau R J, Yamada K, Endoh Y and Shirane G 1997 *Science* **277** 1067
[11] Lee Y S, Birgeneau R J, Kastner M A, Endoh Y, Wakimoto S, Yamada K, Erwin R W, Lee S-H and Shirane G 1999 *Phys. Rev.* B **60** 3643
[12] Mook H A, Dai P, Hayden S M, Aeppli G, Perring T G and Doğan F 1998 *Nature* **395** 580
[13] Valla T, Fedorov A V, Lee J, Davis J C and Gu G D 2006 *Science* **314** 1914
[14] He R H *et al* 2009 *Nat. Phys.* **5** 119
[15] Zhou X J *et al* 2001 *Phys. Rev. Lett.* **86** 5578
[16] Dumm M, Basov D N, Komiya S, Abe Y and Ando Y 2002 *Phys. Rev. Lett.* **88** 147003
[17] Ortolani M, Calvani P, Lupi S, Schade U, Perla A, Fujita M and Yamada K 2006 *Phys. Rev.* B **73** 184508
[18] Castellani C, Di Castro C, Grilli M and Perali A 2000 *Physica* C **341–348** 1739
[19] Homes C C, Dordevic S V, Gu G D, Li Q, Valla T and Tranquada J M 2006 *Phys. Rev. Lett.* **96** 257002
[20] Ando Y, Lavrov A N, Komiya S, Segawa K and Sun X F 2001 *Phys. Rev. Lett.* **87** 017001
[21] Zhou X J *et al* 2003 *Nature* **423** 398
[22] Dumm M, Komiya S, Ando Y and Basov D N 2003 *Phys. Rev. Lett.* **91** 077004
[23] Sutherland M *et al* 2003 *Phys. Rev.* B **67** 174520
[24] Lee Y S, Segawa K, Ando Y and Basov D N 2004 *Phys. Rev.* B **70** 014518
[25] Tohyama T, Nagai S, Shibata Y and Maekawa S 1999 *Phys. Rev. Lett.* **82** 4910

[26] Markiewicz R S 2000 *Phys. Rev.* B **62** 1252
[27] Martin I, Ortiz G, Balatsky A V and Bishop A R 2001 *Europhys. Lett.* **56** 849
[28] Lorenzana J and Seibold G 2003 *Phys. Rev. Lett.* **90** 066404
[29] Millis A J and Norman M R 2007 *Phys. Rev.* B **76** 220503(R)
[30] Lee P A, Nagaosa N and Wen X G 2006 *Rev. Mod. Phys.* **78** 17
[31] Li J X, Mou C Y and Lee T K 2000 *Phys. Rev.* B **62** 640
[32] Berg E, Fradkin E, Kim E-A, Kivelson S A, Oganesyan V, Tranquada J M and Zhang S C 2007 *Phys. Rev. Lett.* **99** 127003